Human stem cell based corneal tissue mimicking structures using laser-assisted 3D bioprinting and functional bioinks

Anni Sorkio [a, b], Lothar Koch [b], Laura Koivusalo [a], Andrea Deiwick [b], Susanna Miettinen [a, d], Boris Chichkov [b, c, 1], Heli Skottman [a, *, 1]

[a] BioMediTech Institute and Faculty of Medicine and Life Sciences, University of Tampere, Arvo Ylpön katu 34, FI-33520 Tampere, Finland
[b] Laser Zentrum Hannover e.V., Hollerithallee 8, 30419 Hannover, Germany
[c] Institute for Quantum Optics, Leibniz Universität Hannover, Welfengarten 1, 30167 Hannover, Germany
[d] Science Center, Tampere University Hospital, P.O. BOX 2000, FI-33521 Tampere, Finland

ABSTRACT

There is a high demand for developing methods to produce more native-like 3D corneal structures. In the present study, we produced 3D cornea-mimicking tissues using human stem cells and laser-assisted bioprinting (LaBP). Human embryonic stem cell derived limbal epithelial stem cells (hESC-LESC) were used as a cell source for printing epithelium-mimicking structures, whereas human adipose tissue derived stem cells (hASCs) were used for constructing layered stroma-mimicking structures.

The development and optimization of functional bioinks was a crucial step towards successful bioprinting of 3D corneal structures. Recombinant human laminin and human sourced collagen I served as the bases for the functional bioinks. We used two previously established LaBP setups based on laser induced forward transfer, with different laser wavelengths and appropriate absorption layers. We bioprinted three types of corneal structures: stratified corneal epithelium using hESC-LESCs, lamellar corneal stroma using alternating acellular layers of bioink and layers with hASCs, and finally structures with both a stromal and epithelial part. The printed constructs were evaluated for their microstructure, cell viability and proliferation, and key protein expression (Ki67, p63α, p40, CK3, CK15, collagen type I, VWF). The 3D printed stromal constructs were also implanted into porcine corneal organ cultures.

Both cell types maintained good viability after printing. Laser-printed hESC-LESCs showed epithelial cell morphology, expression of Ki67 proliferation marker and co-expression of corneal progenitor markers p63α and p40. Importantly, the printed hESC-LESCs formed a stratified epithelium with apical expression of CK3 and basal expression of the progenitor markers. The structure of the 3D bioprinted stroma demonstrated that the hASCs had organized horizontally as in the native corneal stroma and showed positive labeling for collagen I. After 7 days in porcine organ cultures, the 3D bioprinted stromal structures attached to the host tissue with signs of hASCs migration from the printed structure. This is the first study to demonstrate the feasibility of 3D LaBP for corneal applications using human stem cells and successful fabrication of layered 3D bioprinted tissues mimicking the structure of the native corneal tissue.

1. Introduction

The cornea is the transparent anterior part of the eye, which is essential for vision. Corneal blindness due to trauma or diseases affects millions of people worldwide. In the most severe cases, the limbus, a niche for epithelium-renewing limbal epithelial stem cells (LESCs), is destroyed, resulting in limbal stem cell deficiency (LSCD) with overgrowth of the conjunctiva and blood vessels, severe pain and photophobia [1]. In these patients, the traditional corneal transplants from deceased donors have poor long-term success due to lack of epithelial renewal [2,3]. Delivery of *in vitro* expanded autologous LESCs to the corneal surface has been introduced as is a possible treatment for patients suffering from unilateral or partially bilateral LSCD [4,5]. Even more advanced

techniques are required to produce allogeneic LESCs or LESC-like equivalents for bilateral LSCD. Furthermore, the underlying corneal stroma is often damaged especially in cases of traumatic corneal blindness, and requires a replacement to restore visual function. Thus, there is an increased demand for developing methods to produce more native-like 3D corneal structures using human stem cells and functional biomaterials. Tissue engineering has sought to answer this ever-increasing demand by creating chemically defined cell and biomaterial based products to treat and cure corneal blindness.

Biomaterials for corneal stromal reconstruction are required to integrate with the host tissue, be functionally transparent and mechanically stable. For biologically functional corneal tissue equivalents, these materials require a cell density and 3D organization similar to that of the native cornea. Functional corneal stromal tissue has previously been fabricated by seeding human cells into decellularized porcine [6] or human cornea stromal tissue [7] or stimulating human cells to secrete their own extracellular matrix and produce corneal tissue equivalents [8]. However, use of decellularized tissue still lacks established methods for complete removal of antigenic moieties while maintaining proper tissue integrity [9], whereas the tissue equivalents secreted by human cells are slow to manufacture and limited to only thin or stacked constructs [10].

Corneal tissue in general is an optimal target for tissue engineering and 3D bioprinting technology due to its relatively low thickness [11] and lack of vascularization, which has limited the use of 3D printing technology in many other applications, such as bone, heart or skin tissue [12,13]. 3D bioprinting is a promising technique for fast production of thick corneal constructs, but previous work in the field has been conducted with immortalized corneal epithelial cells without any epithelial organization [14]. The applied nozzle-free laser-assisted bioprinting (LaBP) method allows high resolution printing of bioinks with high viscosity and high cell density without affecting the viability of the cells, while being capable of high printing resolution (<10 pL droplets) [15–17]. To reach high resolution with nozzle-based printing techniques, such as extrusion or ink jet printing, small nozzles (<100 μm diameter) are needed, which prevent the use of high cell density due to high shear stress to the cells. Furthermore, with LaBP, we can achieve precise spatial organization of cells and use different cell types in the same engineered structure. In any 3D bioprinting application, a suitable bioink is needed to produce shape-retaining multilayered corneal structures. For production of clinically relevant corneal structures, it is crucial to develop new functional bioinks based on xeno-free components, as well as suitable regenerative cell types.

Human pluripotent stem cells (hPSCs) can provide almost limitless amounts of LESC-like cells, with gene and protein expression similar to native LESCs [18,19]. With our recently established feeder-cell free hPSC culture and differentiation protocol [20], we have further brought our LESC differentiation towards a clinically relevant method for regeneration of the ocular surface. For reconstruction of the corneal stroma, human adipose tissue derived stem cells (hASCs) have gathered wide attention due to their high availability from healthy adult donors, as well as their capability to differentiate towards corneal keratocytes, which has been demonstrated in both *in vitro* [21–23] and *in vivo* [24,25] studies. Furthermore, autologous hASCs have already reached clinical pilots for treating corneal stromal disorders [26]. In addition, hASCs have excellent immunomodulatory properties, reducing inflammation at the site of implantation [27] as well as anti-scarring properties [28,29]. With these two different stem cell types, we can produce a tissue engineered corneal structure, which could simultaneously replace the damaged corneal stroma and regenerate the corneal epithelium.

In the present study, we produced 3D corneal mimicking tissues using human stem cells, functional bioinks and LaBP. Human embryonic stem cell (hESC) derived LESCs were the cell source for printing corneal epithelium-mimicking structures, whereas hASCs were the cellular component in lamellar corneal stromal tissues. We chose human sourced collagen I and recombinant human laminin as bases for the bioinks to develop clinically suitable techniques for corneal tissue engineering. Here, we demonstrate the feasibility of 3D LaBP for corneal applications and show successful fabrication of layered 3D bioprinted tissues from both investigated cell types that resemble the structure of the native corneal tissues.

2. Experimental methods

2.1. Bioinks

For hESC-LESCs, bioink containing human recombinant laminin-521 (LN521; Biolamina, Sweden) was chosen, as laminin is a major component in LESC basement membrane in the native cornea [30]. The hESC-LESC bioink consisted of 33% of 0.1 mg/ml LN521, 50% of defined and serum-free CnT-30 medium (CELLnTEC Advanced Cell Systems AG, Bern, Switzerland) supplemented with RevitaCell™ (100x) (Gibco, Life technologies) at a 1X final concentration, and 17% of 1 w/v% Hyaluronic acid sodium salt (HA) from *Streptococcus equi saline* ($M_w = 1.5–1.8 \times 10^6$ Da) (Sigma Aldrich, Deisenhofen, Germany) in Tris-buffered saline (TBS).

Human collagen I (Col I) was used as a base of the bioink for hASCs as it is the primary component of the human corneal stroma [31]. OptiCol™ Human Collagen Type I (3 mg/ml) (Cell Guidance Systems Ltd, Cambridge, UK) was neutralized to a pH of 7.4 with 0.25 N sodium hydroxide (NaOH) in the presence of 10X Dulbecco's Phosphate Buffered Saline (DPBS, Carl Roth, Karlsruhe, Germany). The bioink for hASCs included 44.4% of neutralized human Col I, 22.2% of ethylenediaminetetraacetic acid (EDTA) human female AB blood plasma, 22.2% of 40 IU/ml Thrombin from human plasma (Sigma Aldrich, Deisenhofen, Germany) in 0.1 M TBS and 11.1% of 10x DBPS. The human plasma was extracted with EDTA tubes, from blood collected from venipunctures and centrifuged at 4500 U/min for 30 min. Thereafter, human plasma was collected and sterile filtrated.

For 3D structures, acellular layers without hASCs were printed between hASCs in order to establish corneal stromal mimicking structures. There, a bioink with 40% of neutralized human Col I, 20% of human plasma, 20% of thrombin, 10% of 1 w/v% HA and 10% of 10x DBPS was used. The specific concentrations for the used reagents are listed above.

2.2. In vitro degradation

Degradation kinetics of the collagen-based hASC bioink in both cell culture medium and varying concentrations of collagenase were determined by weighing the gelled acellular bioink at different time points. For this purpose, the acellular bioink was prepared, as described in Section 2.1, by mixing bioink components to a total volume of 200 μl into 48-wells and allowed to gel for 2–3 h. The gels were then transferred to larger wells for degradation studies in either EBM-2 medium (Lonza, Basel, Switzerland) or in 0.1 M Tris-HCl buffer, pH 7.4, supplemented with 5 mM $CaCl_2$ and 0.005 (w/v) NaN_3, containing 0 U/ml, 5 U/ml, 50 U/ml, or 250 U/ml of collagenase (collagenase type I, CLS I, from *Clostridium histolyticum*; Biochrom, Berlin, Germany) and stored in an incubator at 37 °C. The initial weight of the gels was recorded and they were subsequently weighed at different time points up to 8 days (in medium) or 6 h (in collagenase), respectively. Degradation studies

were performed on four parallel samples at each condition.

2.3. Human embryonic stem cell derived limbal epithelial stem cells

Previously established hESC line Regea08/017 (XX) [32] was used for LESC differentiation as previously described [20]. In brief, undifferentiated hESCs were maintained on well-plates coated with 1.09 µg/cm^2 LN521 in Essential 8™ Flex Medium (E8, Thermo Fisher Scientific) supplemented with 50 U/ml Penicillin-Streptomycin (Gibco, Thermo Fisher Scientific). For LESC differentiation, hESCs were enzymatically detached and transferred to Corning® Costar® Ultra-Low attachment plates in XF-ko-SR medium (KnockOut™ DMEM supplemented with 15% KnockOut™ SR XenoFree CTS™ (XF-ko-SR), 2 mM GlutaMAX™, 0.1 mM 2-Mercaptoethanol, 1% MEM Non-Essential Amino Acids, and 50 U/ml Penicillin-Streptomycin (all from Gibco, Thermo Fisher Scientific)) supplemented with 5 µM blebbistatin (Sigma-Aldrich) overnight to induce embryoid body formation. The following day, the embryoid bodies were guided towards surface ectoderm with one day in XF-ko-SR medium supplemented with 10 µM SB-505124 and 50 ng/ml human basic fibroblast growth factor (PeproTech Inc., Rocky Hill, NJ) followed by two days in XF-ko-SR medium supplemented with 25 ng/ml bone morphogenetic protein 4 (PeproTech Inc.). Subsequently, the embryoid bodies were seeded onto 0.75 µg/cm^2 LN521 and 5 µg/cm^2 collagen IV coated well-plates in CnT-30 medium and cultured for 22–24 days. Finally, differentiated hESC-LESCs were cryopreserved in PSC Cryopreservation Medium (Thermo Fisher Scientific).

For printing, the cryopreserved hESC-LESCs were thawed onto 0.75 µg/cm^2 LN521 and 5 µg/cm^2 human collagen IV coated well plates in CnT-30 medium supplemented with RevitaCell™ (100X) (Gibco, Life technologies) at a 1X final concentration and cultured overnight. The following day, the medium was replaced with CnT-30, and hESC-LESCs were cultured for six to seven days before enzymatically detaching cells with TrypLE™ for printing. After 4 min incubation in TrypLE™, the enzyme was removed, and Defined Trypsin Inhibitor (DTI) (Thermo Fischer Scientific) was added to inactivate any remaining enzyme. Human ESC-LESCs were gently detached with a cell scraper in DTI and centrifuged. Subsequently, the supernatant was removed and cells counted in CnT-30 medium. Appropriate amount of cells was aliquoted in Eppendorf tubes, and centrifuged. The supernatant was removed, and hESC-LESCs were resuspended in LN521 containing bioink and used for LaBP with cell density of 30×10^6 cells/ml.

2.4. Human adipose derived stem cells

Human ASCs were isolated mechanically and enzymatically from subcutaneous adipose tissue samples of a female donor undergoing elective plastic surgery at Tampere University Hospital (Tampere, Finland) according to previously published protocols [33,34]. The isolated hASCs were characterized for their surface marker expression by flow cytometry (FACSAria; BD Biosciences, Erembodegem, Belgium) as previously described [34] (Supplementary Table S1).

The hASCs were cultured in EBM-2 Medium (Lonza, Basel, Switzerland) devoid of fetal bovine serum and supplemented with 2% human serum (type AB male, HIV tested from BioWest, Nuaillé, France). This medium was selected to maintain hASC in their undifferentiated state during *in vitro* culture. Human ASCs were passaged upon confluency using TrypLE™ and used for LaBP at passages 3–5. For printing, hASCs were enzymatically detached with TrypLE™, centrifuged and resuspended in culture medium for counting. Thereafter, hASCs were centrifuged in Eppendorf tubes, supernatant was removed and the cells were resuspended in human Col I based bioink with a cell density of 30×10^6 cells/ml for LaBP.

2.5. Laser-assisted bioprinting of human stem cells

Here, we used laser-assisted bioprinting (LaBP) based on laser induced forward transfer (LIFT). A detailed description of the LaBP setup has been previously published [15]. In brief, the setup consists of a pulsed laser source and two horizontal co-planar glass slides (26×26 mm^2). The upper one, referred to as donor slide, is coated with a thin laser-absorbing layer (two different laser absorbing materials were used in this study) and, subsequently, with a thicker layer of the bioink to be printed. This bioink is usually a sol (the non-gelled precursor of a hydrogel) with embedded cells. The donor slide is mounted upside-down in the printing setup (Supplementary Fig. S1) and laser pulses are focused through the donor slide into the absorption layer, which is evaporated in the laser focus. An expanding vapor bubble is generated at the immobile donor slide surface that propels the subjacent biomaterial towards the second glass slide, referred to as collector slide, or an arbitrary object to print onto. Due to the collapsing of the vapor bubble after a few microseconds and inertia, the bioink forms a jet that lasts for a few hundred microseconds. This jet impinges on the collector slide and deposits as a small droplet in the picoliter volume range (a few ten to a few hundred microns in diameter) on the collector slide. By moving the laser focus, the donor and collector slides relative to each other, bioink droplets are positioned in specific patterns. Thus, 3D structures from the bioink can be produced by repeating this procedure layer-by-layer [35]. The deposition of the bioink is controlled via computerized scanning setup [15]. In this study, we used two laser-based printing systems with different laser wavelengths and appropriate absorption layer material. In the first setup, a Nd:YAG-laser (DIVA II; Thales Laser, Orsay, France) with 1064 nm wavelength, 10 ns pulse duration and 20 Hz repetition rate was combined with a 60 nm thin gold absorption layer. The second system applied an Er:YAG-laser (DPM-15, Pantec Engineering AG, Ruggell, Liechtenstein) with 2940 nm wavelength, 3 µs pulse duration, and up to 1 kHz repetition rate (500 Hz was used within this study); this wavelength fits into an absorption maximum of water making it optimal for hydrogel absorption layers. The first printing setup was applied for printing hESC-LESCs, and hASCs in both 2D and 3D structures, whereas the latter was used for constructing 3D cornea-mimicking structures with both cell types. The laser pulse energy was adjusted for both cell types under investigation. All printing experiments were carried out at room temperature (RT) under humid environment.

For hESC-LESC printing, an additional transparent polyethylene terephthalate (PET) film with 0.4 µm pores (Sarstedt, Nümbrecht, Germany) coated with 0.75 µg/cm^2 LN521 and 5 µg/cm^2 human Collagen IV (Col IV) was placed on the collector glass slide. 50 µl of laminin-containing bioink with hESC-LESCs was spread on the donor layer, resulting in approximate layer thickness of 74 µm. 7 mm × 7 mm samples were printed with a speed of 5000 µm/s. Three layers of hESC-LESCs were printed on top of each other, using laser pulse energy of 18 µJ. The samples were allowed to stabilize at +37 °C for 30 min before adding CnT-30 medium supplemented with 1X RevitaCell™. The following day, the medium was replaced with fresh CnT-30 medium without RevitaCell™. The printed hESC-LESCs were cultured for up to 12 days and the culture medium was changed three times a week.

Human ASCs were printed in 2D patterns in order to evaluate the viability of the cells after LaBP. Collector slides were coated with Corning® Matrigel® Basement Membrane Matrix (Fisher Scientific GmbH, Schwerte, Germany). The Matrigel® was diluted in 2:1 ratio in EBM-2 cell culture medium. 75 µl of diluted Matrigel® was

spread on the collector-slides, and allowed to gel for 10 min at +37 °C. 45 µl of the human Col I containing bioink with hASCs was spread on the donor slide resulting in approximate layer thickness of 67 µm. First, hASCs were printed in lines (with 500 µm spacing), or in spots (with 400 µm spacing) with the speed of 2000 µm/s and laser pulse energy of 20 µJ. The printed samples were allowed to stabilize for 10 min at +37 °C before submerging them in cell culture medium.

For creating 3D corneal stromal mimicking structures, alternating layers of hASCs and acellular layers 7 mm × 7 mm in size were printed with a speed of 5000 µm/s. Laser pulse energy of 20 µJ was used for hASC-containing bioink, while acellular layers were printed with higher laser pulse energy of 25 µJ. 45 µl of the hASC-containing bioink was applied on the donor slide resulting in approximate layer thickness of 67 µm, and 65 µl of the acellular bioink yielded a 96 µm thin layer on the donor slide. Two consecutive layers of hASC-containing bioink were laser-printed, followed by four acellular layers. All cell-containing layers in the 3D bioprinted stromal structures were printed in the same orientation. In total, 10 alternating layers of hASCs and acellular bioink were printed in layer-by-layer manner to create a thick 3D structure, as illustrated in Fig. 1. In total, the 3D laser-printed stromal mimicking structures consisted of 60 printed layers. The 3D stromal mimicking structures were printed on a stabilizing matrix, Matriderm® (Dr. Suwelack Skin & Health Care, Billerbeck, Germany). Matriderm® sheets are nontransparent collagen-elastin matrixes with 1 mm thickness. Matriderm® sheets have been previously used as a stabilizing matrix for Col-based bioinks and hASCs in skin applications [15]. The structures were allowed to stabilize at +37 °C in humid environment for 1 h before submerging them in the EBM-2 culture medium. Thereafter, the printed stromal structures were cultured for 14 days and fresh medium was changed three times a week.

Finally, we combined the two cell types to establish a proof-of-concept for 3D bioprinting human corneal mimicking structures from human stem cells. For this, the second bioprinting system based on LaBP was used in combination with a laser absorption layer composed of 18 µl Matrigel® and 2 µl glycerol, blade coated on a glass donor slide. Matrigel® was chosen, since Matrigel® gels relatively quickly at +37 °C, possess a hydrophilic surface and is biocompatible, while glycerol avoids fast drying of the layer before the bioink is applied on top. The applied human Col I-based bioink gelates very slowly and is thus not optimal as laser absorption layer. The concentration of Matrigel® in the final printed construct was approximately 0.4 µl/cm². On top of the absorption layer, 50 µl of bioink with suspended cells was spread (for printing, the donor

slide was turned upside-down). Laser pulse energies of 150 µJ were applied, which are not directly comparable to those of the first bioprinting setup due to the different wavelength, laser pulse duration, and absorption material. Again, 7 × 7 mm² samples were printed, here with a speed of 7000 µm/s and 100 µm line spacing. The same cell densities and bioinks described above were used for both hESC-LESCs and hASCs. The 3D corneal mimicking structures were allowed to stabilize at +37 °C for 1 h before submerging them in culture medium. For these samples, a medium consisting of 1:1 ratio of CnT-30 with 1X RevitaCell™ and EBM-2 with 2% HS was used. Both PET and Matriderm® sheets were used as stabilizing substrates. The next day, same medium without RevitaCell™ was changed, and the structures were cultured for up to 3 days.

2.6. Cell viability

Cell viability and proliferation of both hESC-LESCs and hASCs after LaBP were assessed with two commercially available assays – LIVE/DEAD® Viability/Cytotoxicity Kit for mammalian cells and PrestoBlue™ cell viability reagent (both from Thermo Fischer Scientific), according to manufacturer's instructions. The hESC-LESC viability with LIVE/DEAD® kit was determined after 3 and 7 days of printing, whereas cell viability of hASCs was analyzed the following day. PrestoBlue™ viability assay was performed at days 1 and 7 for hESC-LESCs, at days 1 and 4 for hASCs printed in 2D patterns, and at days 1, 4 and 7 for hASCs printed in 3D stromal mimicking structures. For hESC-LESCs, eight samples with four technical replicates were analyzed in each time point. For hASCs printed in 2D patterns, in total 20 samples with four technical replicates were analyzed in both time points. Finally, four to six 3D bioprinted stromas with hASCs with four technical replicates were included in cell proliferation analysis at each time point. Moreover, cell morphology was inspected daily with phase contrast microscope.

2.7. Indirect immunofluorescence staining

The cell migration, cell morphology, expression of cell specific markers and tissue structure after LaBP were investigated with immunofluorescence (IF) stainings. For hESC-LESCs and hASCs printed in 2D patterns, the IF staining was done as previously described [36]. Primary antibodies rabbit anti-Ki67 1:200 (Millipore), rabbit anti-p63α 1:200 (Cell Signaling Tech), mouse anti-p40 1:200 (Biocare Medical), mouse anti-CK3 1:200 (Abcam) and mouse anti-CK15 (Thermo Fischer Scientific) were investigated for hESC-LESCs. Primary antibody detection was done with Alexa-Fluor conjugated 488 donkey anti-mouse IgG, 488 donkey anti-rabbit IgG and 568 donkey anti-rabbit IgG (all from Molecular Probes, Life Technologies). All secondary antibodies were diluted 1:400. Phalloidin-Atto 550 1:100 (Sigma Aldrich) was used for visualizing the filamentous actin cytoskeleton of the cells and mounting medium containing 4′,6-diamidino-2-phenylindole (DAPI; Vecta-Shield, Vector Laboratories Inc., Burlingame, CA) was used for staining the nuclei.

The 3D bioprinted structures as well as human corneal samples were rinsed twice with DPBS, and fixed in 4% PFA for 1 h at RT. Subsequently, the 3D samples were rinsed with PBS and incubated in 20% sucrose solution overnight at +4 °C. The next day, the samples were embedded in Tissue-Tek OCT (Science Services, Munich, Germany) and snap frozen at −80 °C. For IF and other histological stainings, cryosections of 7 µm were prepared and air dried for 1 h at RT. Thereafter, the cryosections were incubated in 3% BSA-PBS and 0.1% Triton-X-100 for 1.5 h at +37 °C. Primary antibody dilutions were prepared in 3% BSA-PBS and incubated overnight at +4 °C under humid conditions: rabbit anti-Ki67 1:200
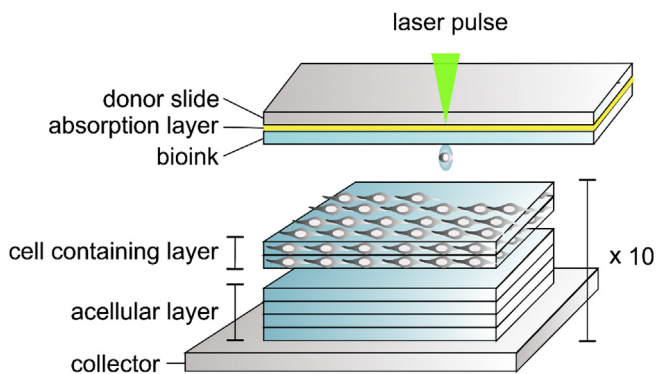

Fig. 1. Schematic diagram of the laser-assisted bioprinting system and printing of the 3D stromal mimicking structures. Stromal mimics comprised 10 alternating layers of hASCs and acellular bioink, with each individual cell-containing layer consisting of two layers of hASCs and the acellular layer consisting of four printed layers.

(Millipore), mouse anti-collagen type I 1:200 (Abcam), rabbit anti-von Willebrand Factor (VWF) 1:200 (Dako Cytomation) and mouse anti-p40 1:200 were used. Primary antibody detection was done with the same secondary antibodies as described above 1:400 in 3% BSA-DPBS for 1.5 h at $+37\ °C$. In addition, filamentous actin was stained with Phalloidin Tetramethylrhodamine B isothiocyanate 1:400 (Sigma Aldrich). Finally, the samples were thoroughly washed with PBS and mounted with ProLong™ Gold Antifade Mountant (Thermo Fischer Scientific) with DAPI to stain the nuclei.

The IF samples were imaged with AxioScope A1 fluorescence microscope (Carl Zeiss) or LSM 700 confocal microscope (Carl Zeiss, Jena, Germany) and images edited using ZEN 2011 Light Edition (Carl Zeiss) and Corel® Photo-Paint X8.

2.8. Hematoxylin and eosin staining

Hematoxylin and eosin (HE) staining was carried out for sections from the 3D bioprinted structures as well as corneal samples. HE staining was carried out following standard procedures for cryosections and paraffin embedded sections, and observed under a Nikon Eclipse TE200S microscope (Nikon Instruments Europe B.V., Amstelveen, Netherlands).

2.9. Corneal organ cultures

The corneal organ culture using excised porcine corneas was conducted as previously described [37—39]. Briefly, fresh porcine eyes were stripped of excess tissue and disinfected with 2% povidone iodine (Betadine®, Leiras, Helsinki, Finland), and the corneas were dissected from the eyes in aseptic conditions. The corneas were cultured partially submerged in CnT-Prime-CC medium (CELLnTECH Advanced Cell Systems AG) supplemented with 1% Penicillin-Streptomycin, 0.25 μg/ml amphotericin B (Thermo Fisher Scientific) and 5 μg/ml Plasmocin (InvivoGen, Toulouse, France) at $+37\ °C$ in 5% CO_2 for two weeks prior to implantation of the 3D bioprinted stromal constructs.

Two-day-old 3D printed stromal structures on the Matriderm® substrate were shipped from Germany to Finland overnight at $+37\ °C$ in EBM-2 medium containing 20 mM HEPES, and implanted into the corneal organ cultures 4 days after printing. Implantation was performed on a Barron artificial anterior chamber (Katena products Inc., Denville, NJ, USA), to allow handling of the cornea during the operation. Corneal epithelium was scraped off using a scalpel (Feather Safety Razor co., ltd, Osaka, Japan), and a 5 mm trephine (Robbins Instruments, Chatham, NJ, USA) was used to make a partial thickness cut to the center of the cornea. The stromal tissue was removed from the trephined area using a crescent knife (Bauch&Lomb Inc., Rochester, NY, USA). The trephine was also used to punch out a 5 mm diameter piece from the 3D printed stromal construct, which was placed into the stromal wound bed with the bioprinted stromal side facing downwards. Matriderm® substrate alone and acellular bulk-formed bioink gels were implanted as negative controls. Although constructs did not withstand suturing in place, it was deemed unnecessary due to the static culture conditions and the fitted trephination of the implant and the wound site. After implantation, the corneas were moved from the artificial anterior chamber back into culture plates, covered with soft contact lenses (EyeQ One-Day Premium, Cooper Vision, Hamble, UK), and cultured partially submerged in EBM-2 medium with 2% HS for 7 days, at $+37\ °C$ in 5% CO_2.

One week after implantation, the corneal organ cultures were fixed in 4% PFA for 4 h at RT, dehydrated in Tissue-Tek VIP 5 (Sakura Finetek Europe) automatic tissue processor overnight, and embedded in paraffin. The paraffin blocks were sectioned into 6-μm-thick slices using a microtome, and the sections were mounted on TOMO® adhesion microscope slides (Matsunami Glass Ind., Ltd., Osaka, Japan).

2.10. Immunohistochemical staining

The corneal organ cultures containing 3D bioprinted stromal constructs and their Matriderm® controls, were analyzed using immunohistochemical staining against the human cell marker TRA-1-85 to detect hASCs in the samples. The staining was performed similarly as in Ref. [40], with slight modifications. Briefly, samples were deparaffinized and hydrated, followed by antigen retrieval in hot 0.01 M citrate buffer (pH 6.0) for 10 min. Tissue intrinsic peroxide activity was blocked by incubation in 0.3% H2O2 for 30 min at RT. Ready-to-use 2.5% normal horse serum (Vector ImmPress reagent, Vector Laboratories Inc.) was used to block unspecific binding. Samples were then labeled with anti-TRA-1-85 mouse IgG antibody (courtesy of Peter Andrews, University of Sheffield) in a 1:100 (v/v) dilution in 0.5% BSA overnight at $+4\ °C$, and labeled with Vector ImmPress horse anti-mouse IgG (containing horseradish peroxidase) (Vector Laboratories Inc.) for 30 min at RT. Staining was visualized by peroxidation reaction with DAB+ chromogen system (Dako North America, Inc., Carpinteria, CA, USA), which was performed for 30 s at RT. The tissue was counterstained using Harris' hematoxylin, followed by dehydration, and mounting using Pertex (Histolab, Askim, Sweden). Samples were imaged using Nikon Eclipse TE200S microscope.

2.11. Statistical analysis

The statistical significance of PrestoBlue™ cell proliferation data was determined with Mann−Whitney U test. The mean values of cell proliferation data for all printed tissues are presented ±standard error. p-values ≤ 0.05 were considered statistically significant. The statistical data analysis was carried out with IBM SPSS Statistics software.

2.12. Ethical issues

This study was carried out under an approval from the local ethics committee of the Pirkanmaa hospital district Finland that allows us to derive and expand hESC lines from surplus embryos donated by couples undergoing infertility treatments, and to use these cell lines for research purposes (R05116). In addition, we have ethical approvals to extract and use hASC for research purposes (R15161) and to use human donor corneas unsuitable for transplantation for research purposes (R11134). New cell lines were not derived for this study.

3. Results

3.1. Laser-printed hESC-LESCs remain viable, express key markers and form mature 3D cornea-like tissue

Initially, laser-printed hESC-LESCs were spherical in morphology (Supplementary Fig. S2) but recovered their normal polygonal morphology during culture. The viability of hESC-LESCs was analyzed with LIVE/DEAD® after 1 and 7 days of printing. In both investigated time points, the laser-printed hESC-LESCs were viable in LN521 containing bioink, with only a few dead cells after 7 days of culture (Fig. 2A). In addition, laser-printed hESC-LESCs showed polygonal epithelial cell morphology at day 7 (Fig. 2B). Significantly higher cell proliferation (p < 0.05) was detected at day 7 after printing compared to cell proliferation at day 1 (Fig. 2C), as confirmed with PrestoBlue™ assay. To verify the cell phenotype and organization, IF staining was carried out at day 7. Phalloidin
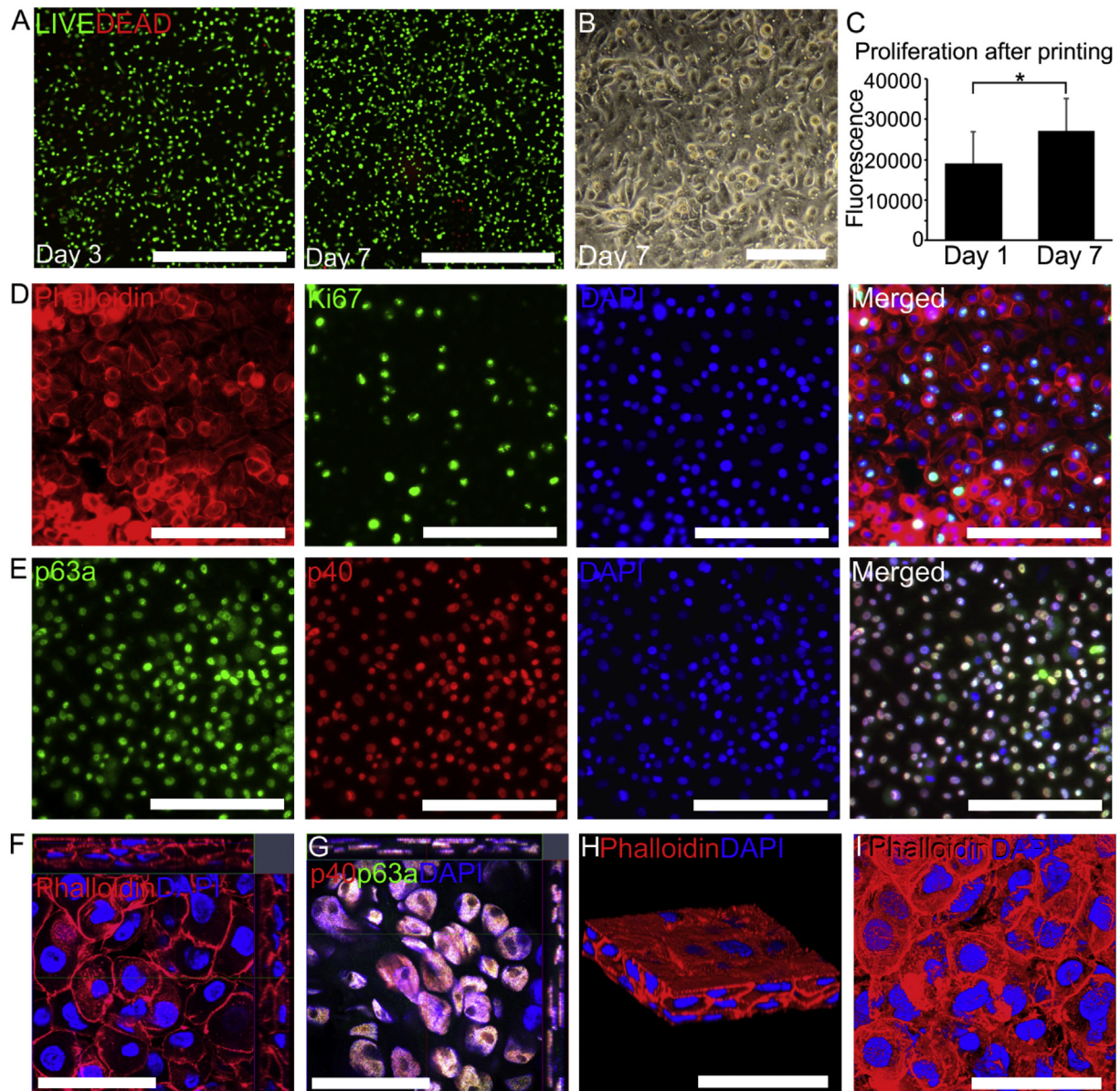
Fig. 2. 3D laser-assisted bioprinting of hESC-LESCs. Cell viability of hESC-LESCs three and seven days after printing shown with live-dead-staining (**A**). Live cells are visualized with green and dead cells with red. Scale bars 1 mm. Phase microscope image of printed hESC-LESCs (**B**). Scale bar 200 μm. Human ESC-LESC proliferation after printing (*p < 0.01) (**C**). Immunofluorescence staining of phalloidin (red) and Ki67 (green) illustrating hESC-LESC cell morphology and proliferating cells after seven days of printing (**D**). Protein expression of corneal epithelial progenitor markers p63α (green) and p40 (red) in 3D bioprinted hESC-LESCs at day seven (**E**). Representative vertical confocal image of layered hESC-LESCs (**F**). Localization of corneal progenitor markers p63α (green) and p40 (red) in layered hESC-LESCs (**G**). 3D rotated (**H**) and top view (**I**) transparency rendering mode confocal images of the layered hESC-LESCs. Scale bars 200 μm (**D-E**) and 50 μm (**F-I**). The nuclei are visualized with DAPI (blue). (For interpretation of the references to colour in this figure legend, the reader is referred to the Web version of this article.)

staining of the actin cytoskeleton confirmed the polygonal epithelial cell morphology of the printed cells seen in phase contrast microscopy (Fig. 2D). Moreover, the printed hESC-LESCs expressed the proliferation marker Ki67 (Fig. 2D) and co-expressed corneal progenitor markers p63α and p40 (Fig. 2E). Importantly, the printed layers of hESC-LESCs retained epithelium-like structure with 3–4 cell layers (Fig. 2F) and with p63α and p40 expressed throughout the layered epithelium (Fig. 2G). Finally, 3D confocal imaging of the day 7 IF samples demonstrated that the hESC-LESCs retained the 3D epithelial tissue after printing (Fig. 2H and I). Conversely, stratified epithelial tissue formation was not observed for non-bioprinted hESC-LESCs seeded in suspension on PET substrates after 7 days (Supplementary Fig. S3).

The 3D bioprinted hESC-LESCs were further cultured up to 12 days, and subsequently analyzed for maturation with IF. At this time point, the 3D bioprinted hESC-LESCs demonstrated epithelial cell morphology (Fig. 3A). Only a few of the printed cells expressed the proliferation marker Ki67 (Fig. 3A), but expression of corneal progenitor markers p63α, p40 and CK15 was strong (Fig. 3B and C). Epithelial cell morphology was also seen in phase contrast micro-scopy (Fig. 3D). Notably, hESC-LESCs showed maturation towards corneal epithelial cells, with expression of CK3, a marker for terminally differentiated corneal epithelium (Fig. 3E). After 12 days, the printed cells retained a stratified epithelium with four distin-guishable cell layers (Fig. 3F–J). The stratified structure of the printed epithelium also demonstrated signs of further maturation
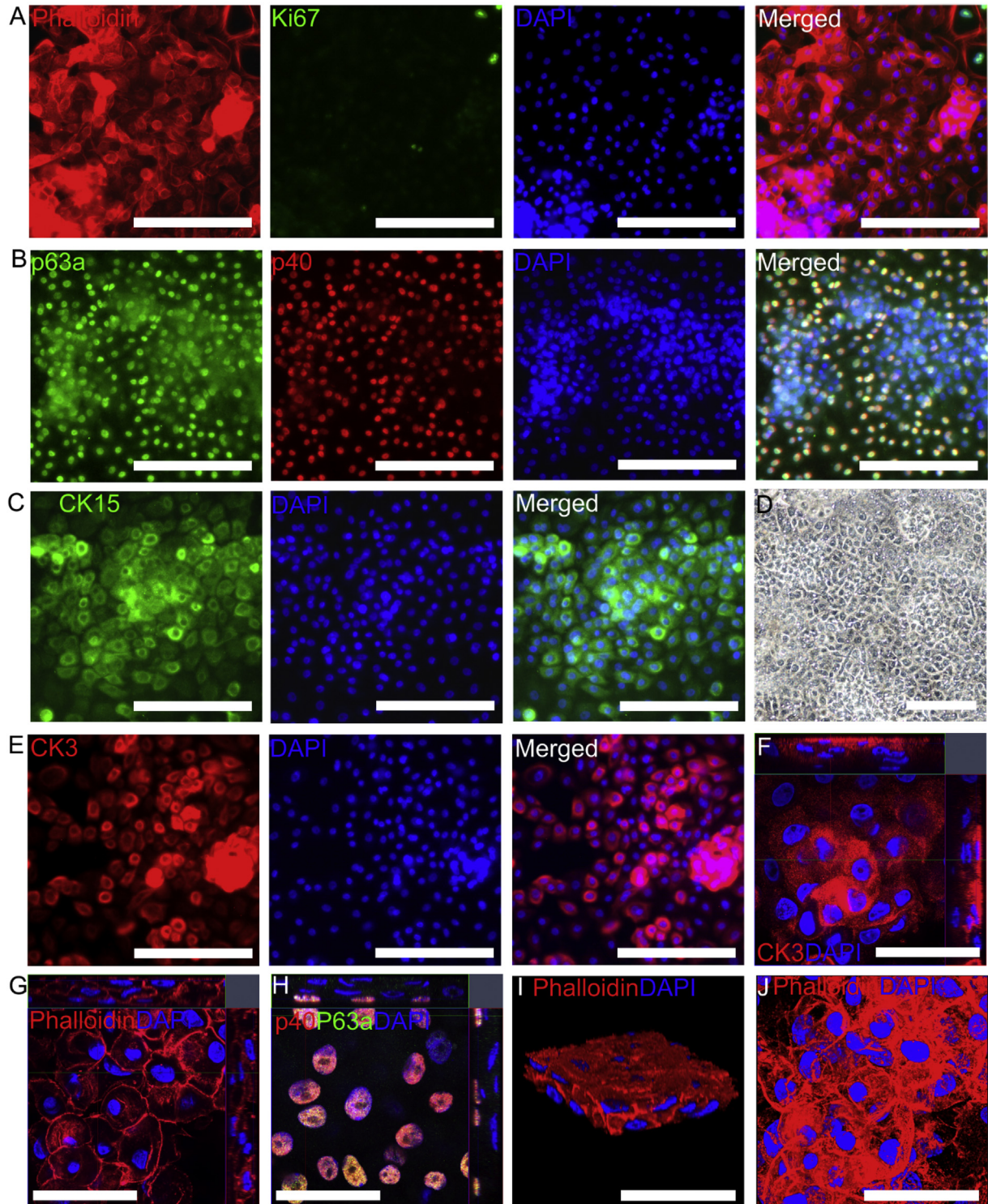
Fig. 3. The maturation of 3D bioprinted hESC-LESCs after 12 days demonstrated with immunofluorescence stainings. **A.** Cell morphology (phalloidin = red) and proliferating cells (Ki67 = green). Expression of corneal progenitor markers p63α (green), p40 (red) (**B**) and CK15 (green) (**C**). Phase microscope image of hESC-LESCs (**D**). Expression (**E**) and apical localization (**F**) of CK3 (red), a marker of terminally differentiated corneal epithelium. Representative vertical confocal sections of the layered hESC-LESCs (**G**) and the basal localization of the corneal progenitor markers p63α and p40 (**H**). 3D rotated (**I**) and top view (**J**) transparency rendering mode confocal images of the layered hESC-LESCs. Scale bars 200 μm (**A-E**) and 50 μm (**F-J**). (DAPI = blue). (For interpretation of the references to colour in this figure legend, the reader is referred to the Web version of this article.)

when analyzed with confocal microscopy, with apical expression of CK3 (Fig. 3F) and basal expression of p63α and p40 (Fig. 3H). The 3D confocal imaging confirmed the 3D epithelial tissue-like structure 12 days after printing (Fig. 3I and J).

3.2. hASCs in human Col I based bioink remain viable and proliferate after LaBP

The biocompatibility of human Col I-containing bioink after

LaBP was first investigated by printing hASC in organized 2D patterns of aligned lines and spots. The human Col I containing bioink with hASCs demonstrated good printability and biocompatibility. The cells demonstrated excellent viability 1 day after printing: hardly any dead cells were detected in LIVE/DEAD® analysis of hASCs printed in lines (Fig. 4A) and spots (Fig. 4B). Cell viability was further confirmed with PrestoBlue™ and IF. The hASCs printed in line pattern showed significantly higher cell proliferation (p < 0.001) at day 4 compared to day 1. Both printed patterns were clearly visible on day 1 after printing, with elongated cells migrating from both patterns (Fig. 4D and E). By day 4, the initial printed patterns were not visible anymore, as the cells had proliferated and migrated extensively. However, hASCs printed in 2D lines clearly organized in a uniformly aligned fashion by day 4. Finally, hASCs printed in both patterns expressed cell proliferation marker Ki67 at both time points (Fig. 4D and E).

3.3. Laser-printed hASCs form organized corneal stromal mimicking structures

LaBP was used for fabricating thicker 3D stromal structures from hASCs and human Col I-containing bioink. Alternating layers of hASC-containing bioink and acellular bioink were printed to mimic the lamellar structure of the human corneal stroma, with each layer printed with the same orientation (Fig. 1). Initially, the 3D structures had an approximate thickness of 500 μm in a base area of 7 mm × 7 mm. The viability of the 3D printed structures was studied with PrestoBlue™ and LIVE/DEAD® staining. Human ASCs in 3D structures showed significantly higher cell proliferation (p < 0.001) after 4 and 7 days of culture compared to day 1 (Fig. 5A). Moreover, cell proliferation increased significantly (p < 0.05) between 4 and 7 days of culture. LIVE/DEAD® analysis of the 3D bioprinted structures demonstrated high cell viability after printing, with the majority of the cells viable throughout the structures (Fig. 5B and C). Only a few dead cells were detected when viewing the structures from the top (Fig. 5B), although slightly more dead cells were seen in the lower part of the structure when examining the cross-section (Fig. 5C). After 4 days of culture, Ki67 expressing cells were detected in IF analysis of the frozen sections (Fig. 5D), confirming the survival and viability of hASCs in 3D bioprinted structures. Without Matriderm® supportive sheets as a printing substrate, the printed structures showed extensive shrinkage and lost their printed form after a few days of culture.

The structure and cellular organization of the 3D bioprinted grafts were visualized from frozen sections with IF stainings (Fig. 5E–I) and compared to the structure of the native human corneal stroma (Fig. 5J and L). In all investigated time points, the hASCs had organized sparsely throughout the 3D structure. Moreover, some lamellar structures had formed, and hASCs showed elongated cell morphology. Even though the 3D bioprinted structures had higher cell density, the cell organization in 3D printed structures resembled the native human corneal stroma. Furthermore, high-magnification confocal images demonstrated that the hASCs had organized horizontally (Fig. 5K) as in the native corneal stroma (Fig. 5L). The thickness of the printed structures decreased slightly in culture: after 14 days, structures with thickness of 300 μm remained. When analyzing the cell organization in the printed structures from the top, a clear orientation of the cells was detected (Fig. 5M and N). The hASCs in the outermost layer were organized as an aligned cell layer (Fig. 5M), with almost perpendicular orientation to the layer directly underneath (Fig. 5N). 3D confocal images of the printed corneal stromal mimicking structures also confirmed the cellular organization into lamellae (Fig. 5O) with aligned cells (Fig. 5P). In addition, HE staining of the frozen cross-section of 3D bioprinted grafts after 7 days (Fig. 5Q)

demonstrated the lamellar structure of the matrix and cells similar to the human corneal stroma (Fig. 5R).

The slight decrease in thickness of the bioprinted stromal constructs can be related to the loss of mass from the bioinks observed in the *in vitro* degradation data, which indicated that the bioink lost roughly half of its mass after 8 days in medium (Supplementary Fig. S4A). In the presence of 250 U/ml collagenase, the bioink degraded completely in only 4 h, but degradation was slower in more dilute collagenase concentrations (Supplementary Fig. S4B).

Finally, the matrix organization and composition of the 3D bioprinted structures were studied from the frozen cross-sections with IF staining and confocal imaging 7 days after printing. The 3D bioprinted structures showed positive labeling for collagen I and VWF, indicating that the surrounding matrix of the hASCs is mainly composed of human Col I and human plasma (Fig. 6A). High magnification confocal images from the frozen cross-sections showed horizontal and fibrillary alignment of these matrix proteins in the printed structures (Fig. 6B).

3.4. 3D bioprinted stromal structures show interaction and attachment to host tissue in corneal organ culture

The functionality of 3D bioprinted corneal stroma mimicking structures with hASCs was assessed using excised porcine corneas. Large stromal wounds were inflicted, where 3D bioprinted structures were implanted 4 days after printing. Matriderm® supportive sheets without hASCs were used as a control. In addition, the effect of acellular bioink alone was studied in the corneal organ culture. After 7 days in porcine corneal organ cultures, the 3D bioprinted structures showed interaction and attachment to the host tissue (Fig. 7A). Moreover, TRA-1-85 positive cells were detected in the host stromal tissue, indicating possible cell migration of hASCs from the printed structure (Fig. 7B). Strong adhesion of the printed tissue to the host corneal stroma was also revealed (Fig. 7C). The Matriderm® sheets alone and acellular bioink without hASCs showed only minor interaction with the host stroma (Fig. 7D–G). In contrast to the Matriderm-containing bioprinted constructs, the acellular bioink showed evidence of porcine epithelium overgrowth (Fig. 7G–I).

3.5. Laser-printed corneas from human stem cells resemble the structure of native corneal tissue

Finally, we tested a proof-of-concept to fabricate tissue-engineered cornea using both investigated human stem cell types. Multiple layers of hESC-LESCs were printed on top of the thicker 3D stromal structures containing hASCs. The corneal structure printed using the Matrigel™ absorption layer showed moderate transparency when printed on transparent PET substrate (Fig. 8A). However, printing on non-transparent Matriderm® supportive sheets was required to prevent the structure from shrinking during culture (Fig. 8B). After 3 days of co-culture, the hESC-LESCs showed a stratified, corneal progenitor marker p40 positive, layer on the surface of the laser-printed structures (Fig. 8C). The transparency of the constructs did not change during culture. The thickness and structure of the printed epithelium in tissue-engineered corneas resembled the structure of the uppermost part of the native human cornea used as a control.

4. Discussion

3D bioprinting is a promising method for efficient fabrication of the layered cornea-mimicking structures. To our best knowledge, only one previous study has assessed 3D bioprinting for corneal tissue engineering, by using pressure-assisted bioprinting of
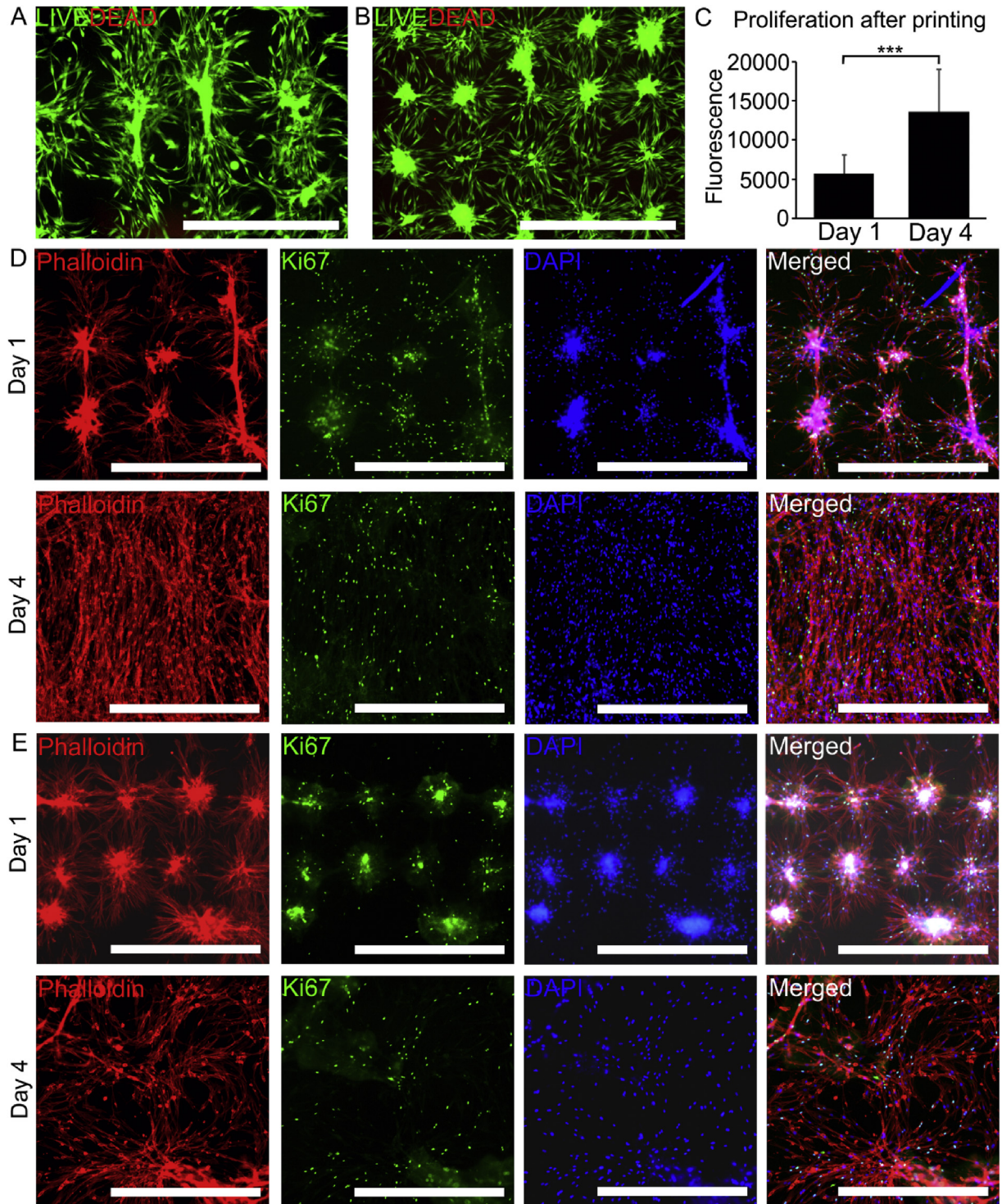
Fig. 4. Laser-assisted bioprinting of hASCs. Viability of hASCs printed as lines (**A**) and spots (**B**) after 1 day of printing. Live cells are shown in green and dead cells with red. Cell proliferation of hASCs printed in lines after one and four days of printing (**C**). Cell morphology and migration (phalloidin = red) and proliferating cells (Ki67 = green) of hASCs printed in lines (**D**) and spots (**E**) at one and four days. Scale bars 1 mm. The nuclei are visualized with DAPI (blue). (For interpretation of the references to colour in this figure legend, the reader is referred to the Web version of this article.)

immortalized human corneal epithelial cells in bioink containing rat-tail Col I, gelatin and alginate [14]. In contrast, our approach utilizes clinically relevant bioinks and two different human stem cell types with potential for corneal regeneration. In this study, we demonstrate the use of LaBP for producing native-like 3D cornea-mimicking structures using human stem cells and functional biomaterials. We developed novel bioinks from recombinant and human sourced materials for constructing 3D bioprinted corneal epithelium-mimicking structures from hESC-LESCs and stroma-mimicking structures from hASCs. Finally, we also tested a proof-of-concept to fabricate a tissue-engineered cornea using both stem cell types. To our knowledge, this is the first study to exploit
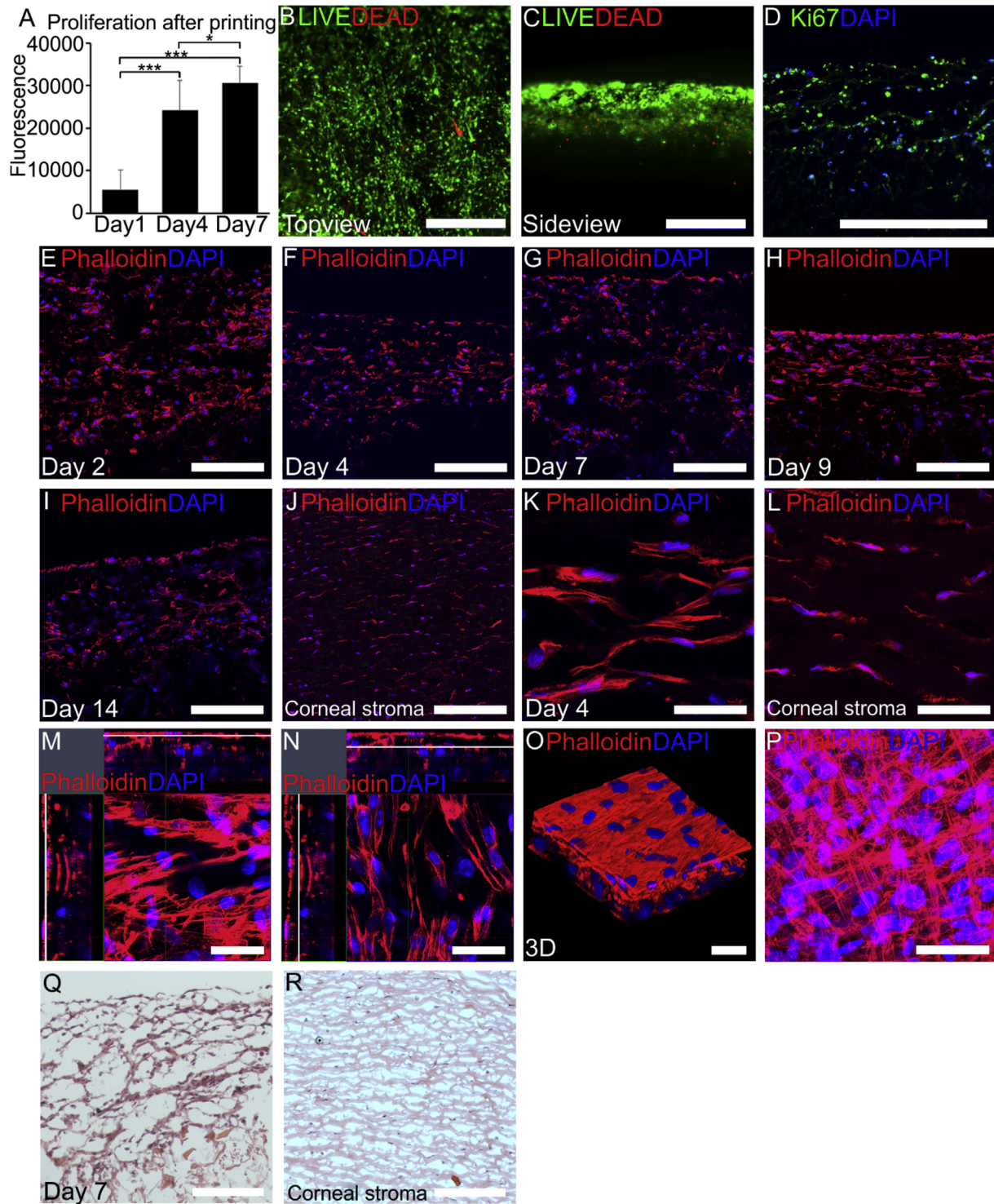
Fig. 5. Constructing 3D corneal stroma mimicking structures using hASCs and laser-assisted bioprinting. Cell proliferation of hASCs in 3D bioprinted structure 1, 4 and 7 days after printing (**A**) (***p < 0.001 and *p < 0.01). Top-view (**B**) and cross-section (**C**) of the live/dead-staining demonstrating the cell viability of hASCs in 3D the following day after printing (live cells = green, dead cells = red). Proliferating cells (Ki67 = green) visualized with immunofluorescence staining from cryosection after four days of printing (**D**). Scale bars 500 μm (**B-D**). Human ASC distribution, morphology and orientation in 3D bioprinted structures visualized with phalloidin (red) from cryocross-Sections 2 days (**E**), 4 days (**F**), 7 days (**G**), 9 days (**H**) and 14 days (**I**) after printing. The human corneal stroma is shown as a control (**J**). Scale bars 200 μm (**E-J**). High-magnification confocal images of the cell orientation in 3D bioprinted stroma after four days since printing (**K**) and in human corneal stroma (**L**). Vertical confocal sections of hASC in 3D bioprinted layered structure: cell orientation in the 1st layer (**M**) and 2nd layer (**N**). 3D rotated confocal image (**O**) and confocal maximum intensity projection image (**P**) of the top-layers in the 3D bioprinted stroma 7 days after printing. Scale bars 50 μm (**K-P**). Hematoxylin and eosin staining of 3D bioprinted stroma at 7 days (**Q**) and central human corneal stroma (**R**). Scale bars 200 μm (**Q-R**). (DAPI = blue). (For interpretation of the references to colour in this figure legend, the reader is referred to the Web version of this article.)
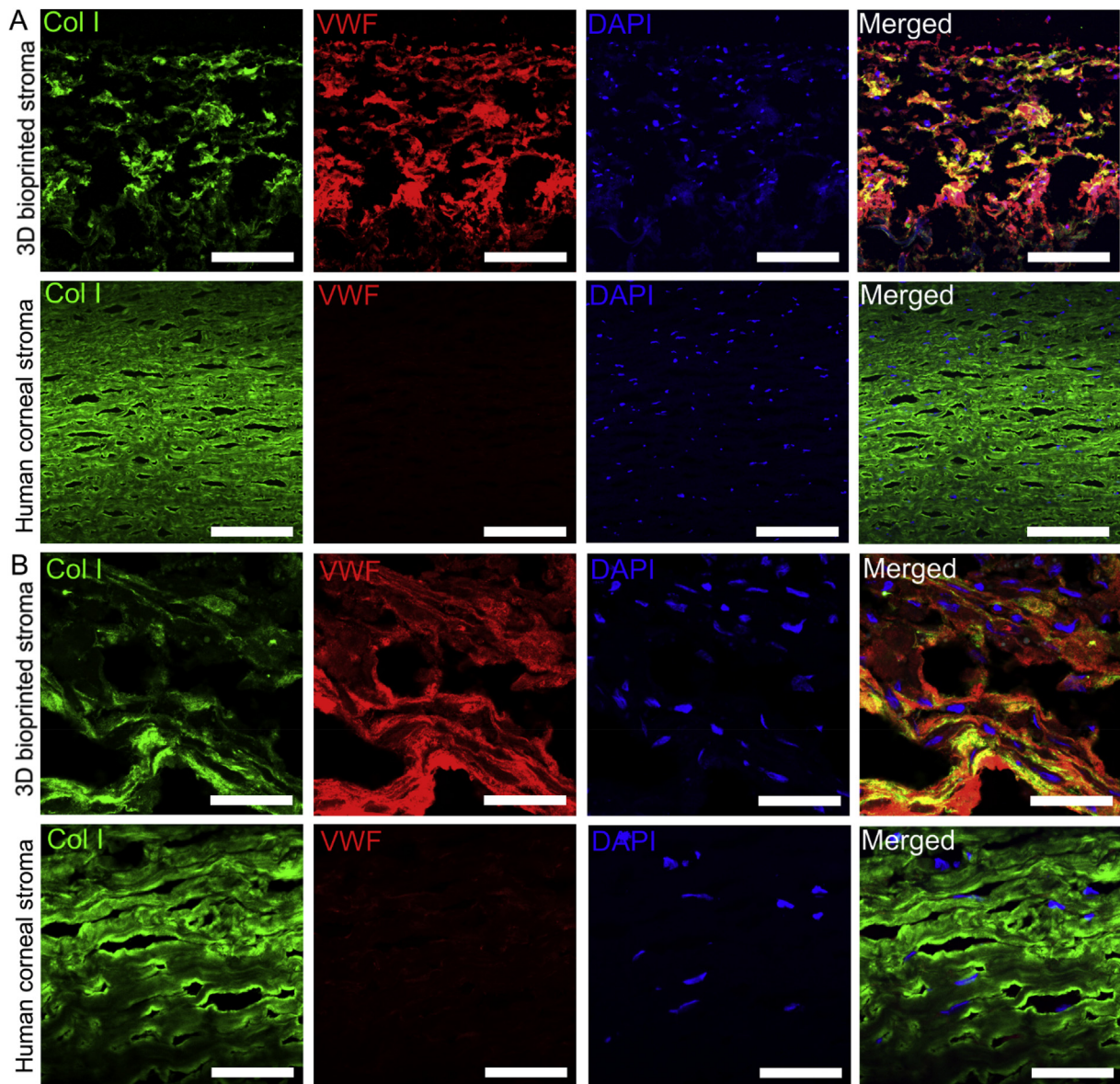
Fig. 6. Matrix composition of 3D bioprinted stroma 7 days after printing. Immunofluorescence staining of cryocross-sections against human collagen I (Col I, green) and Von Willebrandt factor (VWF, red) with low (**A**) and high (**B**) magnification confocal images. Human corneal stroma was used as a control. Scale bars 200 μm. (For interpretation of the references to colour in this figure legend, the reader is referred to the Web version of this article.)

LaBP for corneal tissue engineering applications.

LaBP with LIFT offers advantages over many other 3D bio-printing technologies, such as printing high-resolution 3D structures from viscous bioinks [41,42]. With LaBP, we can also achieve precise spatial organization of cells and use different cell types in the same engineered construct. Previous studies have shown successful bioprinting of both human induced pluripotent stem cells (hiPSC) and hESCs using extrusion-based bioprinting platforms [43—45]. These studies have shown that undifferentiated hPSCs can be bioprinted without adversely affecting their biological functions such as viability, proliferation, and pluripotency [44,45]. The results presented in this study are also among the first to describe successful 3D bioprinting of hPSC-derived cells, as only one previous work has presented printing of hPSC-derived hepatocyte-like cells using a valve-based bioprinting process [44].

In this study, we introduced novel bioinks for 3D bioprinting that show biocompatibility with human stem cells. For the basis of these bioinks, we chose natural components of the LESC basement membrane and corneal extracellular matrix: human recombinant laminin for printing hESC-LESCs, and human Col I for hASCs. Neither recombinant laminin nor human collagen have been previously used as major components of bioinks in 3D bioprinting. However, recombinant laminin-511 (LN511) and LN521 in the form of protein coatings have been shown to enhance the *in vitro* adhesion, migration, and proliferation of human limbal epithelial cells [46], and LN521 is used in combination with Col IV for differentiation of hESC-LESCs [20]. Col I is the major structural protein of the corneal stroma, where it exists as highly arranged fibrils [47]. Due to its major structural role in the native human corneal stroma, collagen has been vigorously investigated for corneal bioengineering [31]. Recently, human Col I and medical grade Col I bioengineered matrices have shown some promise in corneal tissue engineering applications [48,49]. In addition, porcine Col I has been investigated for use in corneal implants [19,50—52] In general, Col I
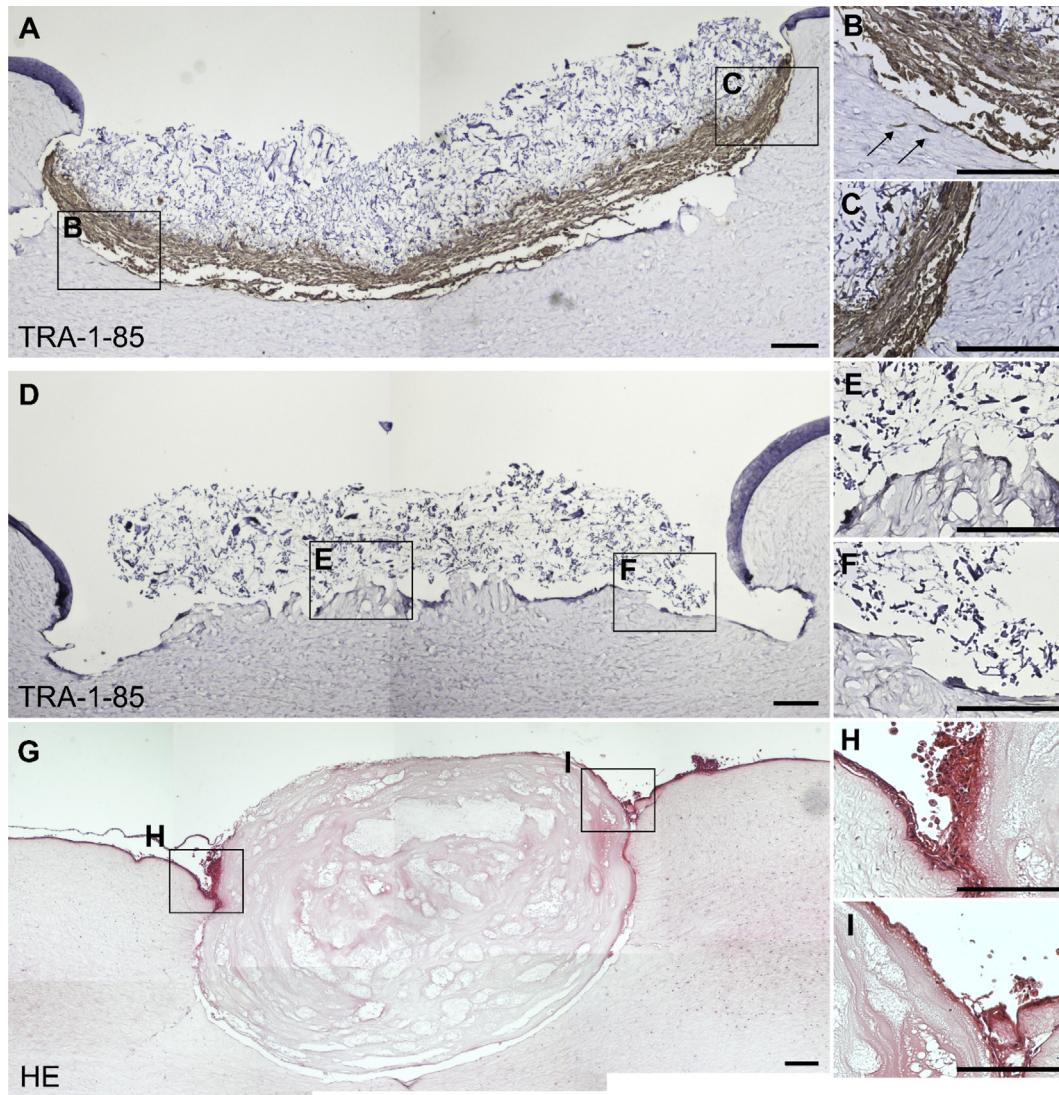
Fig. 7. 3D bioprinted stroma in porcine corneal organ culture model after 7 days (**A-C**). Blank Matriderm® sheets (**D-F**) and acellular bioink were used as control (**G-I**). Immunohistochemical staining of human cell marker TRA-1-85 (brown) demonstrated successful hASC integration into the porcine corneal stroma from the 3D bioprinted stromal mimicking structures, whereas for Matriderm® and acellular bioink only minor interaction with the stroma were observed. HE staining of the acellular bioink in organ culture showed evidence of overgrowth of the porcine epithelium. Scale bars 200 μm. (For interpretation of the references to colour in this figure legend, the reader is referred to the Web version of this article.)

from animal sources, such as rat tail and bovine, have been extensively used in 3D bioprinting in various applications (reviewed in Refs. [35,53—55]). However, it has been previously demonstrated that Col I from different sources show different ultrastructure and biomaterial properties and that the human Col I requires special handling upon biomaterial fabrication compared to bovine Col I [56]. Thus, results and fabrication parameters gained with animal-derived Col I in 3D bioprinting applications are not directly transferrable to use with the more clinically relevant human Col I. Here, we demonstrated the printability and biocompatibility of both LN521 and Col I based bioinks in LaBP.

Usually, bioinks require rapid crosslinking after 3D bioprinting to develop self-supporting structures that maintain their desired shape upon fabrication and in further culture [57]. In this study, we produced stable 3D cornea-mimicking structures without further crosslinking. For printing of hESC-LESCs, we utilized high viscosity bioinks achieved through mixing of HA and cell culture medium to LN521. The structures maintained their shape due to high viscosity

caused by the presence of HA as well as high cell density. Despite the lack of further crosslinking, the printed hESC-LESCs formed 3D epithelium-mimicking tissue, which maintained its structure in culture. Sufficient stability for 3D bioprinted stromal structure from Col I bioink and hASCs was established with human blood plasma and thrombin coagulation during printing. Previously, the fibrin-thrombin coagulation reaction has been utilized for production of biomaterials for primary LESC culture and transplantation [58], and stabilization of 3D bioprinted skin [55,59]. In addition, gelatin/fibrin composite scaffolds stabilized in thrombin solution have been shown to sustain 14 days of culture, although both gelatin and fibrin are bioresorbable and degrade enzymatically [60]. Notably, the printed stromal mimicking structures showed extensive shrinkage and lost their original form after a few days of culture, unless printed on a Matriderm® supportive sheet. Even with the Matriderm® supportive sheets, the thickness of the printed structures decreased in culture: after 14 days, structures with thickness of 300 μm remained suggesting that further crosslinking of the Col I
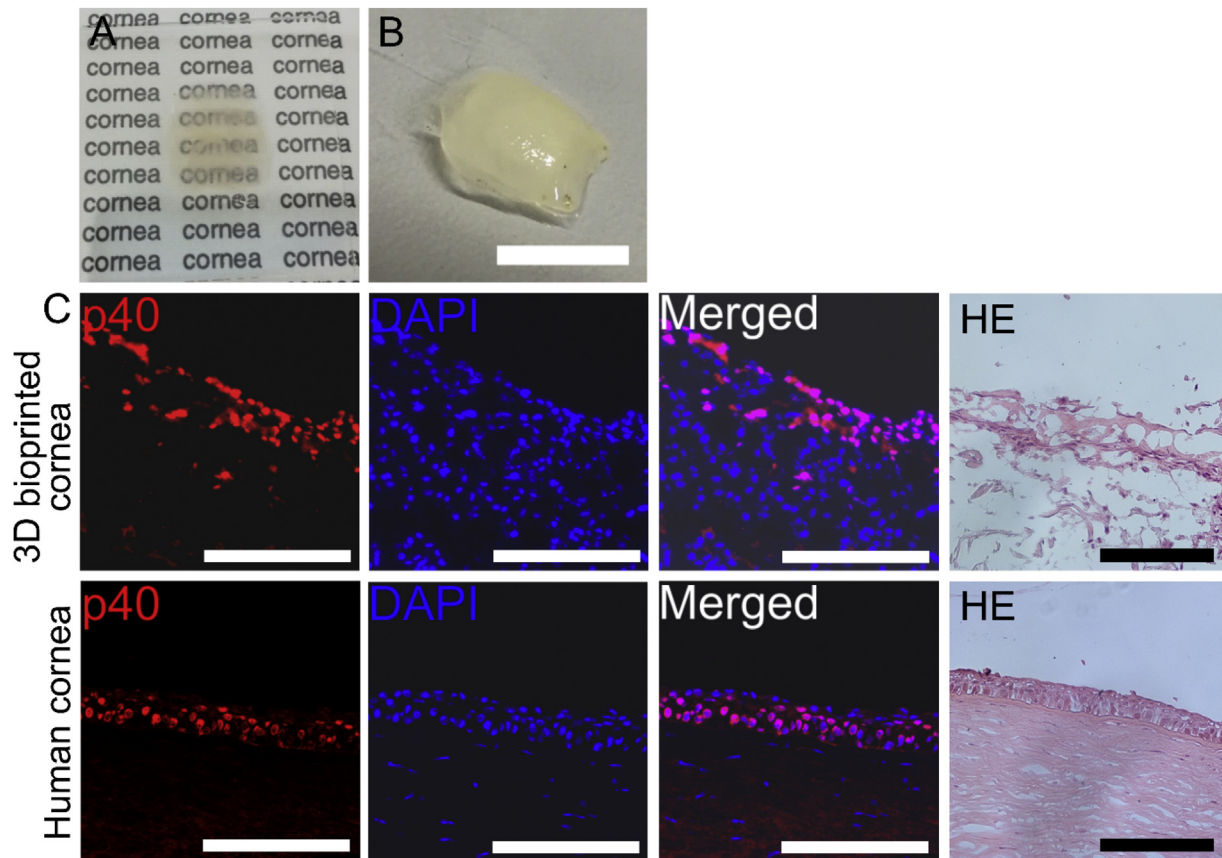
Fig. 8. 3D cornea from hESC-LESCs and hASCs fabricated using laser-assisted bioprinting. The bioprinted 3D cornea fabricated on PET substrate (**A**) shows moderate transparency, however printing on non-transparent Matriderm® substrate (**B**) was required to avoid shrinkage of the structure during culture. **C** shows comparison between the 3D bioprinted corneal tissue and the native human cornea. Immunofluorescence staining of cryocross-sections show multilayered structure of corneal progenitor marker p40 (red) positive hESC-LESCs on top of 3D scaffold after two days since printing. Hematoxylin and eosin (HE)-staining shows the structure of the bioprinted tissue. Cryosections of human cornea were used as a control. Scale bars in **B** 10 mm and in **C** 200 μm. (For interpretation of the references to colour in this figure legend, the reader is referred to the Web version of this article.)

bioink after LaBP might be needed to gain sufficient stability and mechanical stiffness. In order for the crosslinking not to obstruct the LaBP, the crosslinking should be induced after suspending cells. Photo-crosslinking of the printed corneal construct is one option to increase the mechanical stiffness of the printed grafts. However, it should be noted that these crosslinking methods require the addition of a photo-initiators or chemical crosslinkers that could be cytotoxic and may reduce cell survival in the 3D printed grafts [61,62].

The structures fabricated by LaBP showed high resolution after printing as well as functional cell maturation during culture. Initial printability and biocompatibility studies of human Col I containing bioink for printing hASC revealed cell organization in clearly visible 2D patterns with good cell viability. By day 4 in culture, the initial printed patterns were not visible anymore, and cells showed high proliferation marker expression, elongated cell morphology with some degree of alignment. In the bioprinted epithelium-mimicking structures, hESC-LESCs also maintained high viability and proliferation after printing, and showed typical polygonal epithelial cell morphology, and high expression of corneal progenitor markers p63α and p40. Importantly, the printed hESC-LESCs maintained their bioprinted 3D epithelial tissue structure with 3—4 cell layers and showed notable maturation towards corneal epithelium with apical expression of CK3 and basal expression of p63α and p40 within 12 days of culture. However, further studies are required to fully address the functionality of the hESC-LESC formed epithelium after 3D bioprinting.

Formation of the corneal stromal mimicking structures was achieved by bioprinting alternating layers of hASC-containing bioink and acellular bioink. Human ASCs had organized uniformly throughout the 3D structures and showed high proliferation and viability after printing. Although the 3D bioprinted structures had higher cell density than the native corneal stroma, the achieved cell organization in 3D printed structures was similar. In future studies, achieving more native like cell densities of corneal stroma could be realized through optimization of bioprinting parameters such as layer organization and thickness. The high-magnification confocal images revealed that the hASCs had organized in layers with alternating alignment, as in the native corneal stroma. Furthermore, these structures showed positive labeling for collagen I and VWF, indicating horizontal and fibrillar alignment of human Col I and plasma in the printed structures. Interestingly, these fibers demonstrated some organization and arrangement in the 3D environment, indicating that 3D bioprinting with LaBP is a promising fabrication method for corneal stromal mimicking structures. Previously, lamellar collagen organization has been achieved by culturing primary corneal stromal cells on aligned templates, but these methods are time-consuming and resulting structures limited in thickness [8,10,63]. As we did not crosslink the Col I matrix during fabrication, the fiber-like Col I seen after printing was likely produced or remodeled by the printed hASCs in the 3D structure. This could indicate functionality of these cells, as one of the key functions of corneal stromal cells is to produce and modify collagen fibers to maintain the fine stromal architecture [31].

However, further studies are needed to fully address the functionality of the hASCs, their collagen production and ECM remodeling with respect to the printed layer thickness in the 3D structure.

To assess the functionality of the 3D bioprinted stromal mimicking structures with hASC, we implanted them into organ-cultured porcine corneas. 7 days after implantation, the 3D bioprinted stromal structures showed interaction and attachment to the host tissue. Moreover, TRA-1-85 positive human cells were detected in the host stromal tissue, indicating potential cell migration of hASCs from the printed structure. In contrast, the Matridem® sheet alone showed only modest interaction with the stroma. Acellular bioink, on the other hand, showed evidence of overgrowth of host epithelium indicating good biocompatibility of the bioink. Importantly, successful implantation to the corneal organ culture model demonstrated good mechanical robustness of the 3D bioprinted structures, as they could withstand shipping from Germany to Finland, as well as mechanical handling during the implantation operation. Although additional means of fixing the implants in place were not used, the implanted hASCs showed attachment to the stromal wound bed. However, further development is required to achieve better surgically feasible structures, focusing on finding suitable transfer substrates instead of the Matriderm® sheets.

In the final stage, we tested a proof-of-concept to fabricate tissue-engineered cornea using both investigated human stem cell types. We bioprinted layers of hESC-LESCs on top of the thicker 3D stromal structures containing hASCs, and the resulting structures resembled the uppermost part of the native cornea. After 3 days of culture, the hESC-LESCs retained a corneal progenitor marker p40 positive layered epithelium, with four to six cell layers. However, the co-culture conditions of these two cell types need to be developed further [64,65] to enable longer culture periods *in vitro*, while maintaining the corneal regenerative properties of both cell types. For advanced *in vitro* functionality studies, such as barrier properties and mechanical studies of the bioprinted corneal structures, controlled differentiation and maturation towards corneal stroma and epithelium in different layers of the printed constructs are required. Importantly, new substrates for the bioprinted corneal structures are needed for optimizing both transparency and stability of the structures for proper realization of clinically feasible bioprinted corneal grafts.

5. Conclusions

With this study, we demonstrate for the first time the feasibility of 3D LaBP for corneal applications using human stem cells, and show successful fabrication of layered 3D bioprinted tissues mimicking the structure of native corneal tissues. In addition, we introduce novel human protein based bioinks for 3D bioprinting that show biocompatibility with human stem cells. The fabricated 3D corneal structures also demonstrated good mechanical properties without additional bioink crosslinking after LaBP. The *in vitro* and *in vivo* functionality of the 3D structures requires further studies but feasibility of the approach shows promise in porcine corneal organ culture.

Roles for all authors

AS: Conceived and designed the experiments, performed the experiments, analyzed and interpreted the data, wrote the manuscript; **LKoc**: Conceived, designed, and performed experiments, contributed to the writing of the manuscript and its critical revision and final approval; **LKoi**: Conceived and designed the experiments, performed the experiments, analyzed and interpreted the data, wrote the manuscript; **AD:** Contributed regents/materials/analysis

tools, performed experiments, participated in the critical revision of the manuscript; **SM**: Contributed regents/materials/analysis tools, participated in the critical revision of the manuscript; **BC**: Organized and supervised laser printing experiments, participated in the critical revision of the manuscript and final approval of the article; **HS**: Acquired the funding, conceived and designed the experiments, interpreted the data; participated in the critical revision of the manuscript and final approval of the article.

Data availability statement

The raw/processed data required to reproduce these findings cannot be shared at this time due to technical or time limitations but will be available to download from http://www.biomeditech.fi/research/eye-regeneration-group/

Acknowledgements

Appendix A. Supplementary data

Supplementary data related to this article can be found at https://doi.org/10.1016/j.biomaterials.2018.04.034.

References

[1] M. Haagdorens, S.I. Van Acker, V. Van Gerwen, S.N. Dhubhghaill, C. Koppen, M. Tassignon, et al., Limbal stem cell deficiency, current treatment options and emerging therapies, In Vivo 11 (2015) 14.
[2] Y. Oie, K. Nishida, Corneal regenerative medicine, Regen. Ther. 5 (2016) 40–45.
[3] G. Pellegrini, P. Rama, S. Matuska, A. Lambiase, S. Bonini, A. Pocobelli, et al., Biological parameters determining the clinical outcome of autologous cultures of limbal stem cells, Regen. Med. 8 (2013) 553–567.
[4] P. Rama, S. Matuska, G. Paganoni, A. Spinelli, M. De Luca, G. Pellegrini, Limbal stem-cell therapy and long-term corneal regeneration, N. Engl. J. Med. 363 (2010) 147–155.
[5] G. Pellegrini, A. Lambiase, C. Macaluso, A. Pocobelli, S. Deng, G.M. Cavallini, et al., From discovery to approval of an advanced therapy medicinal product-containing stem cells, in the EU, Regen. Med. 11 (2016) 407–420.
[6] E. Yoeruek, T. Bayyoud, C. Maurus, J. Hofmann, M.S. Spitzer, K. Bartz-Schmidt, et al., Decellularization of porcine corneas and repopulation with human corneal cells for tissue-engineered xenografts, Acta Ophthalmol. 90 (2012).
[7] M.A. Shafiq, R.A. Gemeinhart, B.Y. Yue, A.R. Djalilian, Decellularized human cornea for reconstructing the corneal epithelium and anterior stroma, Tissue Eng. C Meth. 18 (2011) 340–348.
[8] R.M. Gouveia, V. Castelletto, I.W. Hamley, C.J. Connon, New self-assembling multifunctional templates for the biofabrication and controlled self-release of cultured tissue, Tissue Eng. A 21 (2015) 1772–1784.
[9] A.P. Lynch, M. Ahearne, Strategies for developing decellularized corneal scaffolds, Exp. Eye Res. 108 (2013) 42–47.
[10] R.M. Gouveia, E. González-Andrades, J.C. Cardona, C. González-Gallardo, A.M. Ionescu, I. Garzon, et al., Controlling the 3D architecture of Self-Lifting Auto-generated Tissue Equivalents (SLATEs) for optimized corneal graft composition and stability, Biomaterials 121 (2017) 205–219.
[11] C.E. Ghezzi, J. Rnjak-Kovacina, D.L. Kaplan, Corneal tissue engineering: recent advances and future perspectives, Tissue Eng. B Rev. 21 (2015) 278–287.
[12] N. Hong, G. Yang, J. Lee, G. Kim, 3D bioprinting and its in vivo applications,

J. Biomed. Mater. Res. Part B Appl. Biomater. 106B (2018) 444—459.

[13] C.S. Ong, P. Yesantharao, C.Y. Huang, G. Mattson, J. Boktor, T. Fukunishi, et al., 3D bioprinting using stem cells, Pediatr. Res. 83 (2018) 223—231, https://doi.org/10.1038/pr.2017.252.

[14] Z. Wu, X. Su, Y. Xu, B. Kong, W. Sun, S. Mi, Bioprinting three-dimensional cell-laden tissue constructs with controllable degradation, Sci. Rep. 6 (2016) 24474.

[15] L. Koch, S. Kuhn, H. Sorg, M. Gruene, S. Schlie, R. Gaebel, et al., Laser printing of skin cells and human stem cells, Tissue Eng. C Meth. 16 (2009) 847—854.

[16] Y. Lin, Y. Huang, D.B. Chrisey, Droplet formation in matrix-assisted pulsed-laser evaporation direct writing of glycerol-water solution, J. Appl. Phys. 105 (2009), 093111.

[17] H. Jian, M. Wang, S. Wang, A. Wang, S. Bai, 3D bioprinting for cell culture and tissue fabrication, Bio. Des. Manuf. (2018) 1—17.

[18] A. Mikhailova, T. Ilmarinen, H. Uusitalo, H. Skottman, Small-molecule induction promotes corneal epithelial cell differentiation from human induced pluripotent stem cells, Stem Cell Rep. 2 (2014) 219—231.

[19] A. Mikhailova, A. Jylha, J. Rieck, J. Nattinen, T. Ilmarinen, Z. Vereb, et al., Comparative proteomics reveals human pluripotent stem cell-derived limbal epithelial stem cells are similar to native ocular surface epithelial cells, Sci. Rep. 5 (2015) 14684.

[20] H. Hongisto, T. Ilmarinen, M. Vattulainen, A. Mikhailova, H. Skottman, Xeno- and feeder-free differentiation of human pluripotent stem cells to two distinct ocular epithelial cell types using simple modifications of one method, Stem Cell Res. Ther. 8 (2017) 291.

[21] Y. Du, D.S. Roh, M.L. Funderburgh, M.M. Mann, K.G. Marra, J.P. Rubin, et al., Adipose-derived stem cells differentiate to keratocytes in vitro, Mol. Vis. 16 (2010) 2680—2689.

[22] S. Zhang, L. Espandar, K.M. Imhof, B.A. Bunnell, Differentiation of human adipose-derived stem cells along the keratocyte lineage, J. Clin. Exp. Ophthalmol. 4 (2013) 11435.

[23] M. Ahearne, J. Lysaght, A.P. Lynch, Combined influence of basal media and fibroblast growth factor on the expansion and differentiation capabilities of adipose-derived stem cells, Cell Regen. 3 (2014), 13—9769-3-13. eCollection 2014.

[24] F. Arnalich-Montiel, S. Pastor, A. Blazquez-Martinez, J. Fernandez-Delgado, M. Nistal, J.L. Alio del Barrio, et al., Adipose-derived stem cells are a source for cell therapy of the corneal stroma, Stem Cell. 26 (2008) 570—579.

[25] J. Alio del Barrio, M. Chiesa, N. Garagorri, N. Garcia-Urquia, J. Fernandez-Delgado, L. Bataille, et al., Acellular human corneal matrix sheets seeded with human adipose-derived mesenchymal stem cells integrate functionally in an experimental animal model, Exp. Eye Res. 132 (2015) 91—100.

[26] J.L. Alio Del Barrio, M. El Zarif, M.P. de Miguel, A. Azaar, N. Makdissy, W. Harb, et al., Cellular therapy with human autologous adipose-derived adult stem cells for advanced Keratoconus, Cornea 36 (2017) 952—960.

[27] M. Patrikoski, J. Sivula, H. Huhtala, M. Helminen, F. Salo, B. Mannerstrom, et al., Different culture conditions modulate the immunological properties of adipose stem cells, Stem Cells Transl. Med. 3 (2014) 1220—1230.

[28] L. Wang, L. Hu, X. Zhou, Z. Xiong, C. Zhang, H.M. Shehada, et al., Exosomes secreted by human adipose mesenchymal stem cells promote scarless cutaneous repair by regulating extracellular matrix remodelling, Sci. Rep. 7 (2017) 13321.

[29] J. Deng, Y. Shi, Z. Gao, W. Zhang, X. Wu, W. Cao, et al., Inhibition of pathological phenotype of hypertrophic scar fibroblasts via coculture with adipose-derived stem cells, Tissue Eng. A 24 (2018) 382—393.

[30] T. Dietrich-Ntoukas, C. Hofmann-Rummelt, F.E. Kruse, U. Schlotzer-Schrehardt, Comparative analysis of the basement membrane composition of the human limbus epithelium and amniotic membrane epithelium, Cornea 31 (2012) 564—569.

[31] S. Chen, M.J. Mienaltowski, D.E. Birk, Regulation of corneal stroma extracellular matrix assembly, Exp. Eye Res. 133 (2015) 69—80.

[32] H. Skottman, Derivation and characterization of three new human embryonic stem cell lines in Finland, In Vitro Cell. Dev. Biol. Anim. 46 (2010) 206—209.

[33] J.M. Gimble, F. Guilak, Adipose-derived adult stem cells: isolation, characterization, and differentiation potential, Cytotherapy 5 (2003) 362—369.

[34] B. Lindroos, S. Boucher, L. Chase, H. Kuokkanen, H. Huhtala, R. Haataja, et al., Serum-free, xeno-free culture media maintain the proliferation rate and multipotentiality of adipose stem cells in vitro, Cytotherapy 11 (2009) 958—972.

[35] S. Michael, H. Sorg, C. Peck, L. Koch, A. Deiwick, B. Chichkov, et al., Tissue engineered skin substitutes created by laser-assisted bioprinting form skin-like structures in the dorsal skin fold chamber in mice, PLoS One 8 (2013), e57741.

[36] A.E. Sorkio, E.P. Vuorimaa-Laukkanen, H.M. Hakola, H. Liang, T.A. Ujula, J.J. Valle-Delgado, et al., Biomimetic collagen I and IV double layer Langmuir—Schaefer films as microenvironment for human pluripotent stem cell derived retinal pigment epithelial cells, Biomaterials 51 (2015) 257—269.

[37] L. Koivusalo, J. Karvinen, E. Sorsa, I. Jönkkäri, J. Väliaho, P. Kallio, et al., Hydrazone crosslinked hyaluronan-based hydrogels for therapeutic delivery of adipose stem cells to treat corneal defects, Mater. Sci. Eng. C 85 (1 April 2018) 68—78.

[38] C.S. Kamma-Lorger, C. Boote, S. Hayes, J. Albon, M.E. Boulton, K.M. Meek, Collagen ultrastructural changes during stromal wound healing in organ cultured bovine corneas, Exp. Eye Res. 88 (2009) 953—959.

[39] S. Mi, E.P. Dooley, J. Albon, M.E. Boulton, K.M. Meek, C.S. Kamma-Lorger, Adhesion of laser in situ keratomileusis-like flaps in the cornea: effects of crosslinking, stromal fibroblasts, and cytokine treatment, J. Cataract Refract. Surg. 37 (2011) 166—172.

[40] L. Koivusalo, J. Karvinen, E. Sorsa, I. Jönkkäri, J. Väliaho, P. Kallio, et al., Hydrazone crosslinked hyaluronan-based hydrogels for therapeutic delivery of adipose stem cells to treat corneal defects, Mater. Sci. Eng. C 85 (1 April 2018) 68—78.

[41] W. Zhu, X. Ma, M. Gou, D. Mei, K. Zhang, S. Chen, 3D printing of functional biomaterials for tissue engineering, Curr. Opin. Biotechnol. 40 (2016) 103—112.

[42] S.V. Murphy, A. Atala, 3D bioprinting of tissues and organs, Nat. Biotechnol. 32 (2014) 773—785.

[43] A. Faulkner-Jones, S. Greenhough, J.A. King, J. Gardner, A. Courtney, W. Shu, Development of a valve-based cell printer for the formation of human embryonic stem cell spheroid aggregates, Biofabrication 5 (2013), 015013.

[44] A. Faulkner-Jones, C. Fyfe, D. Cornelissen, J. Gardner, J. King, A. Courtney, et al., Bioprinting of human pluripotent stem cells and their directed differentiation into hepatocyte-like cells for the generation of mini-livers in 3D, Biofabrication 7 (2015), 044102.

[45] Q. Gu, E. Tomaskovic-Crook, G.G. Wallace, J.M. Crook, Bioprinting: 3D bioprinting human induced pluripotent stem cell constructs for in situ cell proliferation and successive multilineage differentiation (Adv. Healthcare mater. 17/2017), Adv. Healthc. Mater. 6 (2017).

[46] N. Polisetti, L. Sorokin, N. Okumura, N. Koizumi, S. Kinoshita, F.E. Kruse, et al., Laminin-511 and-521-based matrices for efficient ex vivo-expansion of human limbal epithelial progenitor cells, Sci. Rep. 7 (2017) 5152.

[47] K.M. Meek, C. Knupp, Corneal structure and transparency, Prog. Retin. Eye Res. 49 (2015) 1—16.

[48] N. Vázquez, M. Chacón, C.A. Rodríguez-Barrientos, J. Merayo-Lloves, M. Naveiras, B. Baamonde, et al., Human bone derived collagen for the development of an artificial corneal endothelial graft. In vivo results in a rabbit model, PLoS One 11 (2016), e0167578.

[49] W. Liu, K. Merrett, M. Griffith, P. Fagerholm, S. Dravida, B. Heyne, et al., Recombinant human collagen for tissue engineered corneal substitutes, Biomaterials 29 (2008) 1147—1158.

[50] M. Koulikovska, M. Rafat, G. Petrovski, Z. Veréb, S. Akhtar, P. Fagerholm, et al., Enhanced regeneration of corneal tissue via a bioengineered collagen construct implanted by a nondisruptive surgical technique, Tissue Eng. A 21 (2015) 1116—1130.

[51] M. Rafat, F. Li, P. Fagerholm, N.S. Lagali, M.A. Watsky, R. Munger, et al., PEG-stabilized carbodiimide crosslinked collagen—chitosan hydrogels for corneal tissue engineering, Biomaterials 29 (2008) 3960—3972.

[52] M. Rafat, M. Xeroudaki, M. Koulikovska, P. Sherrell, F. Groth, P. Fagerholm, et al., Composite core-and-skirt collagen hydrogels with differential degradation for corneal therapeutic applications, Biomaterials 83 (2016) 142—155.

[53] M.K. Włodarczyk-Biegun, A. del Campo, 3D bioprinting of structural proteins, Biomaterials 134 (2017) 180—201.

[54] M. Yeo, J. Lee, W. Chun, G.H. Kim, An innovative collagen-based cell-printing method for obtaining human adipose stem cell-laden structures consisting of core—sheath structures for tissue engineering, Biomacromolecules 17 (2016) 1365—1375.

[55] L. Koch, A. Deiwick, S. Schlie, S. Michael, M. Gruene, V. Coger, et al., Skin tissue generation by laser cell printing, Biotechnol. Bioeng. 109 (2012) 1855—1863.

[56] S. Majumdar, Q. Guo, M. Garza-Madrid, X. Calderon-Colon, D. Duan, P. Carbajal, et al., Influence of collagen source on fibrillar architecture and properties of vitrified collagen membranes, J. Biomed. Mater. Res. B Appl. Biomater. 104 (2016) 300—307.

[57] S. Ji, M. Guvendiren, Recent advances in bioink design for 3D bioprinting of tissues and organs, Front. Bioeng. Biotechnol. 5 (2017).

[58] G. Milazzo, D. Ardigo, M. Toschi, S. Matuska, P. Rama, M. De Luca, et al., Holoclar: first of its kind in more ways than one, Cell Gene Ther. Insights 2 (2016) 183—197.

[59] N. Cubo, M. Garcia, J.F. del Cañizo, D. Velasco, J.L. Jorcano, 3D bioprinting of functional human skin: production and in vivo analysis, Biofabrication 9 (2016), 015006.

[60] W. Xu, X. Wang, Y. Yan, W. Zheng, Z. Xiong, F. Lin, et al., Rapid prototyping three-dimensional cell/gelatin/fibrinogen constructs for medical regeneration, J. Bioact. Compat. Polym. 22 (2007) 363—377.

[61] C.G. Williams, A.N. Malik, T.K. Kim, P.N. Manson, J.H. Elisseeff, Variable cytocompatibility of six cell lines with photoinitiators used for polymerizing hydrogels and cell encapsulation, Biomaterials 26 (2005) 1211—1218.

[62] H. Liang, W. Chang, H. Liang, M. Lee, H. Sung, Crosslinking structures of gelatin hydrogels crosslinked with genipin or a water-soluble carbodiimide, J. Appl. Polym. Sci. 91 (2004) 4017—4026.

[63] D. Karamichos, M.L. Funderburgh, A.E. Hutcheon, J.D. Zieske, Y. Du, J. Wu, et al., A role for topographic cues in the organization of collagenous matrix by corneal fibroblasts and stem cells, PLoS One 9 (2014), e86260.

[64] E.A. Gosselin, T. Torregrosa, C.E. Ghezzi, A.C. Mendelsohn, R. Gomes, J.L. Funderburgh, et al., Multi-layered silk film co-culture system for human corneal epithelial and stromal stem cells, J. Tissue Eng. Regen. Med. 12 (1) (January 2018) 285—295.

[65] A.K. Kureshi, M. Dziasko, J.L. Funderburgh, J.T. Daniels, Human corneal stromal stem cells support limbal epithelial cells cultured on RAFT tissue equivalents, Sci. Rep. 5 (2015) 16186.